



# Drying kinetics and mathematical modeling of shredded tobacco under hot air drying

Zhiqi Wang<sup>1</sup> · Qianghui Yi<sup>1</sup> · Xiaoxia Xia<sup>1</sup> · Xin Li<sup>1</sup> · Sifeng Zhang<sup>1</sup> · Xiaoyue Zhang<sup>1</sup>

Received: 25 October 2023 / Accepted: 24 January 2024 / Published online: 11 February 2024  
© The Author(s), under exclusive licence to Springer-Verlag GmbH Germany, part of Springer Nature 2024

## Abstract

In the traditional tobacco drying process, there is often a problem of uneven drying, which is closely related to drying conditions such as air velocity and temperature. To better understand the drying characteristics of tobacco, its drying kinetic performance were experimentally studied and predicted in this paper. In the drying experiment, the range of air temperature and velocity is 20–60°C and 0.95–4.93 m/s, respectively. The results show that the effective diffusion coefficient increases with the increase of air temperature and decreases with the increase of air velocity. The effective moisture diffusivity ( $D_{eff}$ ) ranges from  $2.077 \times 10^{-7}$  to  $9.136 \times 10^{-7}$  m<sup>2</sup>/s. Additionally, the activation energy ( $E_a$ ) is between 14.292 and 21.032 kJ/mol according to Arrhenius law. Among the six commonly used empirical correlations, the logarithmic model has higher prediction accuracy, but it has a prediction deviation of more than 20% in the later stage of drying. Based on the logarithmic model and the two models, a new prediction model of tobacco drying characteristics was proposed with a maximum relative deviation error of less than 1%.

## Nomenclature

$v$	Volume(m <sup>3</sup> )
$D_{eff}$	Effective moisture diffusivity (m <sup>2</sup> /s)
$D_0$	The pre-exponential factor of the Arrhenius equation(m <sup>2</sup> /s)
$n$	The number of terms taken into consideration
$E_a$	Energy of activation (kJ/mol)
$k_1, k_2$	Slop of straight line
$M_e$	Equilibrium moisture content of the sample (kg water/kg dry solid)
$M_0$	The initial moisture content (kg water/kg dry solid)
$M(t)$	The moisture content at any time (kg water/kg dry solid)
$MR$	Moisture ratio
$R_g$	Universal gas constant (8.3143 kJ/mol)
$T_a$	Absolute air temperature (K)
$t$	Drying time(s)
$\phi^2$	Coefficient of determined
$e_{RMSE}$	Mean bias error
$\chi^2$	Chi-square
$R_2$	Correlation coefficient

$T$	Air temperature (°C)
$v$	Air velocity (m/s)
$r_e$	Equal radius (m)
$k, a, b, c, d, e$	Drying constant

## 1 Introduction

China is the largest country in the manufacture and consumption of cigarettes, with more than 300 million smokers, which accounts for more than one-third of the total number of smokers in the world [1]. A large number of smokers and the high daily smoking volume directly contribute to the huge consumption of cigarettes. Therefore, improving the quality of tobacco is a key issue for tobacco enterprises. At present, the main tobacco drying technology mainly includes drum drying and airflow drying [2]. Compared with drum drying, airflow drying has the characteristics of short drying time, wide operating range, high drying efficiency and good expansion effect, which can improve the production efficiency and quality of tobacco. Therefore, the airflow drying method is widely used in tobacco enterprises. However, the variation of temperature and humidity during drying have a great impact on the quality of cigarettes [3]. In order to control moisture content and improve drying efficiency of tobacco in the dryers, it is of great significance to investigate the drying kinetics and modeling of shredded tobacco during the hot airflow drying process.

✉ Zhiqi Wang  
wangzhiqi@xtu.edu.cn

<sup>1</sup> School of Mechanical Engineering and Mechanics, XiangTan University, Xiangtan 411105, Hunan, China

In order to accurately predict the whole drying process of materials, some scholars have proposed different drying models. Drying models are generally divided into three types: theoretical model, semi-empirical model and empirical model [4–7]. Although the theoretical model explains the mechanism of water transfer in detail, it is complicated and difficult to obtain some characteristic parameters, which seriously affects the practical application of the theoretical model. The Lewis model [8], the Logarithmic model [9] and the Midilli Kucuk model [10] are several commonly used semi-empirical models, which have good applicability by combining certain theoretical basis and drying kinetics test. At the same time, the semi-empirical model has the advantage of high prediction accuracy, so it is widely used [11]. Safa et al. [12] studied the drying characteristics of rosemary in Morocco at different air temperatures and air flows, and it was proved that Midilli Kucuk model was the most suitable thin-layer drying model when nine models tried for simulation was calculated for the drying data. Panchariya et al. [13] conducted an experimental study on the drying model of black tea and found that the Lewis model had the best prediction effect. Ashtiani et al. [14] studied the drying characteristics and thermodynamic model of mint leaves through hot wind and infrared drying. They found that the best model for predicting the drying characteristics of mint leaves was the Midilli Kucuk model. Although there are many studies on crop drying characteristics and thermodynamic models, the drying methods and materials have a direct impact on drying kinetics and corresponding models. Li et al. [15] conducted a study on the variations in moisture content of cigarettes at different temperatures and predicted these changes using several empirical models. They found that the Midilli and Kucuk model had the highest prediction accuracy. Based on experimental data on the moisture content of tobacco during drying, Duan et al. [16] reported that the Midilli and Kucuk models exhibited a favorable predictive performance. Xin et al. [17] compared five empirical models of tobacco drying kinetics and found that the predictions of the logarithmic model were more consistent with the experimental data.

Since tobacco is quite different from other plants, some researchers have studied the drying properties of shredded tobacco. For example, Zhu et al. [18] simulated temperature and moisture evolution of shredded tobacco under single-stage and two-stage drying in a dual fixed bed dryer by an established heat and mass transfer model and found it had a good prediction accuracy. Duan et al. [16] studied the temperature-changing drying process of shredded tobacco by experimental equipment and found that the Midilli model could better describe the temperature-changing drying kinetics. However, the effect of airflow speed on the drying process of tobacco was ignored. Gu et al. [19] developed a mathematical model which could describe the heat and mass transfer in a rotary dryer for shredded tobacco. Based

on the numerical simulation method, Nie et al. [20] studied the distribution of temperature, humidity and velocity during the drying process of cut tobacco in a drum, and the research results provided a basis for the structure optimization of the cut tobacco drum. Xie et al. [21] found that the increase of drum wall temperature and hot air temperature led to the increase of thermal working strength in the drying process of tobacco. Liu et al. [22] studied the influence of steam injection position on tobacco quality. Chen et al. [23] experimentally studied the isothermal drying kinetics of three typical tobacco. It is found that isothermal drying can be divided into three processes and deceleration drying is the main process. Jiang [24] simulated the variation of temperature, velocity, and moisture content of tobacco during the drying process in a convective drying equipment.

From the above literature review, although some studies have investigated the drying process of tobacco in the drum, the drying kinetics of tobacco still need to be further studied. In addition, it is not clear which empirical correlation is suitable for predicting the drying characteristics of tobacco. To fill this gap, the drying kinetics and mathematical model of tobacco were studied experimentally in this paper. The drying characteristics of shredded tobacco were predicted by using several selected corrections. Finally, a new prediction correlation was proposed to improve the prediction accuracy of drying characteristics of tobacco. This study contributes to the understanding the drying characteristics of shredded tobacco, which can be used in the design and improvement of drum drying equipment.

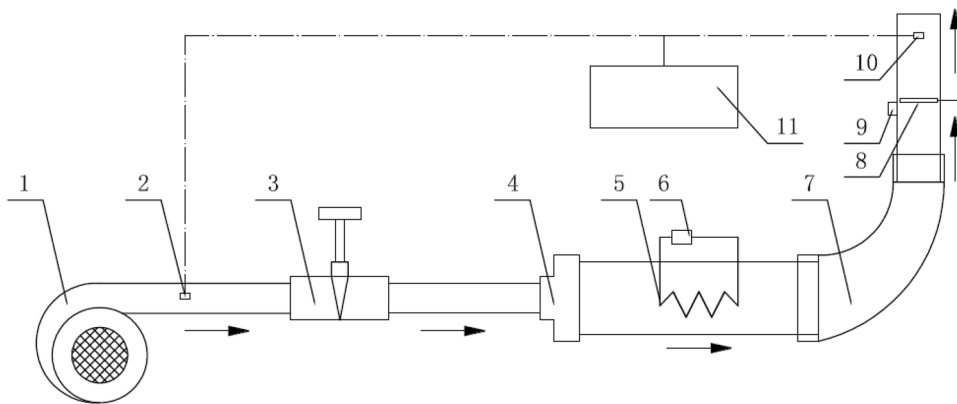
## 2 Materials and methods

### 2.1 Materials and experimental device

The wet shredded tobacco sample was provided by the Tobacco Company in Fujian Province, which had a moisture content of 30% and a density of  $120 \text{ kg/m}^3$  at ambient temperature. To prevent the undesirable effect from the surrounding, the samples were stored in a dry box.

The experimental equipment consists of a hot-air dryer (Fig. 1). The dryer was placed in an environment where the relative air humidity was about 40–50% and the ambient temperature was about 18–22 °C. Air was heated by the electric heater from ambient temperature to the predetermined temperature, then the hot air flowed through the sample and the tobacco was continuously dried. The heating power was regulated by a voltage regulator and the hot air outlet temperature fluctuations were within  $\pm 0.1 \text{ }^\circ\text{C}$ . A FLUKE 923 anemometer enabling  $\pm 0.01 \text{ m/s}$  accuracy was employed to measure the air velocity. An AQ3020Y temperature and humidity sensor with an accuracy of 0.1% was used for measuring temperature and humidity. During

**Fig. 1** Diagram of hot-air dryer: (1) centrifugal fan, (2) inlet air temperature and humidity sensor, (3) flow regulating valve, (4) variable diameter joint, (5) air heater, (6) voltage regulator, (7) variable diameter elbow, (8) sample tray, (9) hot ball anemometer, (10) outlet air temperature and humidity sensor, (11) post-processing computer



the experimental drying process, tobacco weighing was made approximately every 0.5 min through a precision balance with an accuracy of 0.001 g. The experiments continued until the mass of the shredded tobacco between the two weighing was less than 0.001 g in 3 min. At the same time, the connected computer could record the ambient temperature, humidity and the temperature of drying air in the entrance and exit of the dryer chamber.

At the outlet of the drum drying equipment, the velocity of the drying air is generally in the range of 1-6 m/s, and the surface temperature of the tobacco is between 50°C and 60°C [25, 26]. According to the characteristics of the drum drying process, the speed range of drying air in the experiment was set to 0.93 m/s to 4.93 m/s, and its temperature range was set to 20°C to 60°C. During the experiment, tobacco was dried under four air speeds of 0.95, 2.0, 2.65, and 4.93 m/s. At each speed, the drying experiment was carried out at 5 air temperatures of 20, 30, 40, 50 and 60 °C. The experiment was repeated 3 times under all drying conditions, and the arithmetic mean of the experimental results was taken. From the experimental tests, we could study and determine the effect of process variables of the drying air on the effective moisture diffusivity, activation energy and energy consumption of the shredded tobacco drying. Then, the obtained experimental drying curves are approached by three mathematical models.

### 2.2 Theoretical analysis of drying characteristics

Many drying dynamics theories are used to evaluate the drying characteristics of food materials. The most commonly used theory is diffusion theory [27], and the general form of the characteristic drying curve is given by  $f = f(MR)$  [28].

$$f = \frac{\left(-\frac{dM}{dt}\right)_t}{\left(-\frac{dM}{dt}\right)_0} \tag{1}$$

$$MR(t) = \frac{M(t) - M_e}{M_0 - M_e} \tag{2}$$

where  $M(t)$  is the moisture content(kg water/kg dry matter) at a given moment,  $M_0$  is the initial moisture content, and  $M_e$  is the moisture content at the equilibrium time, respectively.

The mechanisms of moisture transport in the spherical body during the falling rate drying period can be mathematically from the Fick’s second law diffusion [29]:

$$\frac{\partial MR}{\partial t} = D_{eff} \nabla^2 MR \tag{3}$$

where  $D_{eff}$  is the effective moisture diffusivity ( $m^2/s$ ),  $t$  is the drying time (s) and  $MR$  is the moisture ratio.

Basing on a constant diffusion coefficient and assuming a uniform initial moisture distribution, negligible temperature gradients, negligible drying shrinkage, the solution can be expressed as:

$$MR = \frac{M(t) - M_e}{M_0 - M_e} = \frac{6}{\pi^2} \sum_{n=1}^{\infty} \frac{1}{n^2} \exp\left(-n^2 \pi^2 \frac{D_{eff} t}{r_0^2}\right) \tag{4}$$

where  $n$  can be a positive integer,  $r_0$  stands for the radius of the sphere which the shredded tobacco sample is assumed as a spherical body in the period of drying.

Volume ( $v$ ) of a piece of shredded tobacco was determined by selecting and weighing 50 pieces of shredded tobacco according to the randomness principle of sample extraction. The equivalent radius of the tobacco was found out by equalizing the volume of a piece of shredded tobacco with the equal volume of a sphere with the radius  $r_e$  as  $2.09 \times 10^{-3}$  m [13].

$$V = \frac{4}{3} \pi r_e^3 \tag{5}$$

When the drying time is considerable, the terms other than the first approach zero, and this equation could be reduced to:

$$MR = \frac{6}{\pi^2} \exp\left(-\pi^2 \frac{D_{eff} t}{r_0^2}\right) \quad (6)$$

Equation (6) is used by several researchers [30, 31] in order to describe the diffusion. In case that the radius ( $r_0$ ) for the duration of the drying process is constant. Equation (6) can be simplified to a straight-line equation as

$$\ln(MR) = \ln\left(\frac{6}{\pi^2}\right) - \left(\pi^2 \frac{D_{eff} t}{r_0^2}\right) \quad (7)$$

where the diffusion coefficient  $k_1$  is obtained from the slope of the plot of  $\ln(MR)$  verse time.

$$k_1 = \pi^2 \frac{D_{eff} t}{r_0^2} \quad (8)$$

$D_{eff}$  varying with temperature and activation energy is calculated by Arrhenius type equation [32]

$$D_{eff} = D_0 \exp\left(-\frac{E_a}{R_g T_a}\right) \quad (9)$$

where  $E_a$  is the activation energy,  $R_g$  is universal gas constant (8.3143 kJ/mol),  $T_a$  is absolute air temperature (K).  $D_0$  is the pre-exponential factor of the Arrhenius equation. Equation (6) can be linearized by applying the logarithms as

$$\ln D_{eff} = \ln D_0 - \frac{1}{T_a} \frac{E_a}{R_g} \quad (10)$$

The  $E_a$  can be calculated from the slope of  $\ln D_{eff}$  versus  $1/T_a$  as shown in Eq. (7)

$$k_2 = \frac{E_a}{R_g} \quad (11)$$

The determination of the drying kinetics was achieved using appropriate software calculation. And linear regression analyses were used to fit the experimental data to the equation in order to obtain correlation ( $R^2$ ).

## 3 Results

### 3.1 Characteristic drying curves

The experimental data for shredded tobacco under hot air drying at different air conditions was analyzed in terms of reduction in moisture ratio with drying time presented in Fig. 2. In the initial stage of drying, the moisture ratio of shredded tobacco decreases rapidly and the drying

rate is high. In the later stage of drying, the moisture ratio of tobacco changes slightly and the drying rate is low. As we can see in Fig. 2(a), when the air temperature increases, the moisture ratio of tobacco decreases rapidly. When air velocity is 0.95 m/s, it takes about 18 min for tobacco to reach the equilibrium at air temperature of 20°C. When air temperature rises to 60°C, the drying time is shortened to 9 min. The reason is that increasing the air temperature is helpful to remove the moisture of tobacco sample faster. As shown in Fig. 2(b)-(d), the variation of moisture ratio of tobacco under different wind speeds is similar. This result is consistent with that reported in the literature [29].

On the other hand, since the water vapor can be effectively taken out of the dryer system by flowing air, the increase in air speed can strengthen convective heat and mass transfer between the tobacco sample and air flow during the drying period. However, the drying speed is mainly restricted by the internal moisture diffusion speed. When the wind speed is too high, it is difficult for the internal moisture to diffuse to the tobacco surface in time. Therefore, as the air speed increases, the moisture content of tobacco will be lower at equilibrium and it will take longer time to the equilibrium state. So it can be clearly found that the influence of air velocity on drying rate is smaller than that of air temperature.

### 3.2 Influence of air parameters on $D_{eff}$

The values of  $D_{eff}$  versus temperature at different air velocities are plotted in Fig. 3. It is obvious that the minimum  $D_{eff}$  belongs to the lowest air temperature of 20 °C in Fig. 3, and the value of  $D_{eff}$  is lower as the air velocity increases. Additionally, the higher the temperature, the greater the effective moisture diffusivity. When the air temperature increases from 20°C to 60°C, the effective diffusivity increases by 1.95 times and 1.76 times at air speed of 0.95 m/s and 4.93 m/s, respectively. The effective diffusion coefficient in the present work is higher than the result of the literature [23], which is mainly in the range of  $0.79 \times 10^{-7}$  m<sup>2</sup>/s to  $1.42 \times 10^{-7}$  m<sup>2</sup>/s. It may be related to the differences in the types and sources of tobacco.

The fitted equation and correlation coefficient of moisture diffusivity are given in Table 1. From Table 1, it can be seen that when the air speed is constant, the effective moisture diffusivity is an exponential function of temperature. And all values of  $R^2$  are greater than 0.9854. The maximum value of the correlation coefficient is 0.998 when the air velocity is 4.93 m/s.

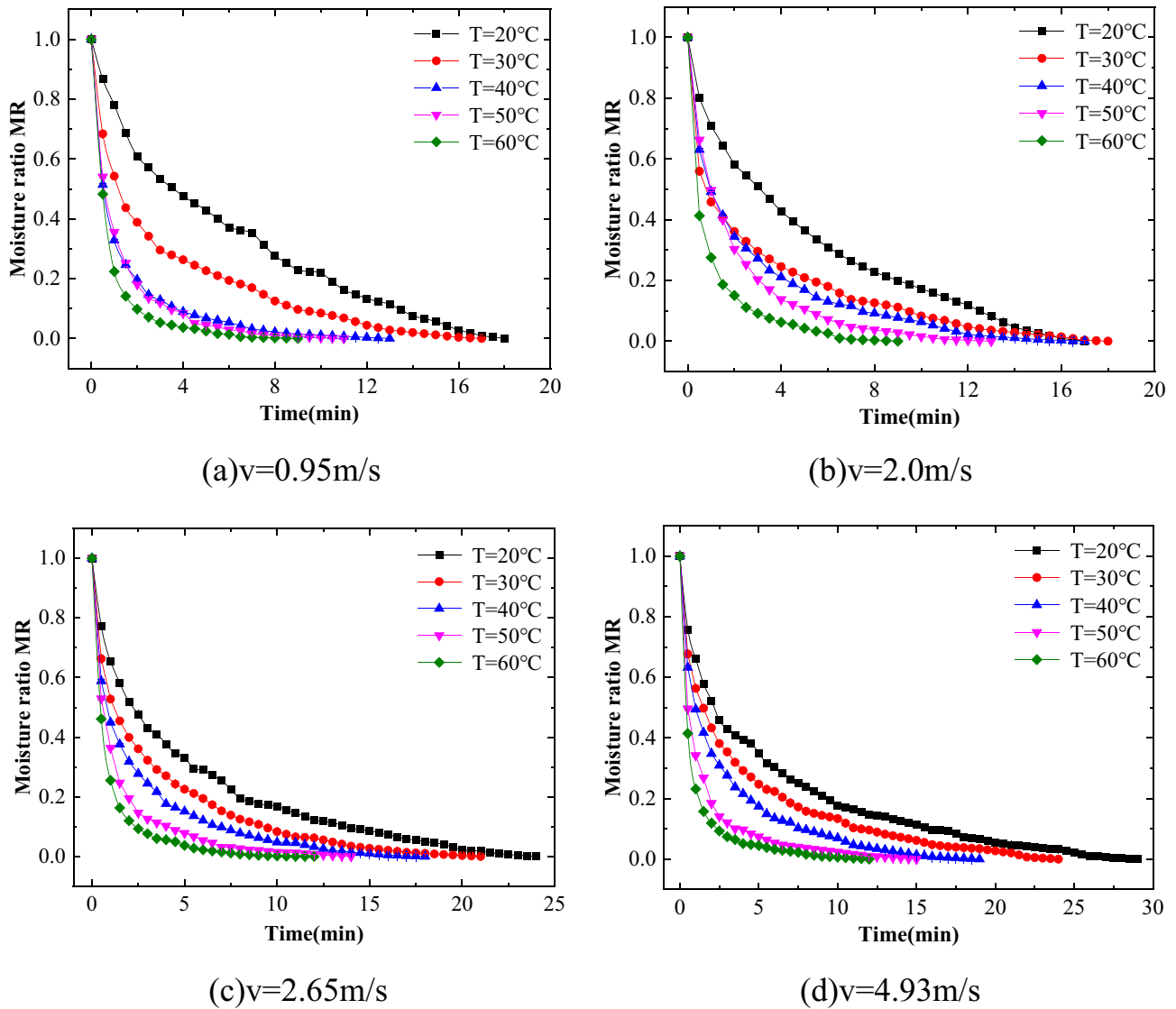


**Fig. 2** Variations of moisture ratio with drying time at different temperatures and air velocities. **a**  $v=0.95$  m/s. **b**  $v=2.0$  m/s. **c**  $v=2.65$  m/s. **d**  $v=4.93$  m/s

Figure 4 shows the values of  $D_{eff}$  versus velocity at different air temperatures. As can be seen in the diagram,  $D_{eff}$  decreases with the increase of air velocity, when the air velocity increases from 0.95 m/s to 4.93 m/s, the effective diffusivity decreases by 34.13%, 33.32%, 33.36%, 37.8% and 38.31% at air temperatures of 20, 30, 40, 50 and 60°C, respectively. The fitted equation and correlation coefficient  $R^2$  under different air temperatures are presented in Table 2. While the air temperature is constant, the effective moisture diffusivity is a quadratic function of the air velocity, and the maximum correlation coefficient is 0.9973 when the air temperature is 30 °C.

Based on multiple regression analysis, the relationship between effective diffusion coefficient and airflow velocity and temperature is shown in Fig. 5. Additionally, the fitted equation for  $D_{eff}$  and the correlation coefficient  $R^2$  are reported as following:

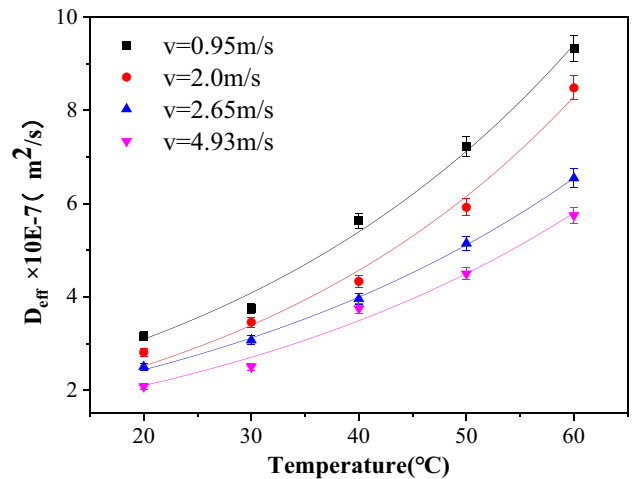


**Fig. 3**  $D_{eff}$  versus temperature at different air velocities for tobacco sample drying

**Table 1** Fitted equation for  $D_{eff}$  value at different air velocities

$v$ (m/s)	Equation $\times 10^{-7}$	$R^2$
0.95	$D_{eff} = 1.738e^{0.0282T}$	0.9884
2.0	$D_{eff} = 1.542e^{0.0275T}$	0.9854
2.65	$D_{eff} = 1.506e^{0.0244T}$	0.9984
4.93	$D_{eff} = 1.217e^{0.0262T}$	0.9980

**Table 2** Fitted equation for  $D_{eff}$  value at different air temperatures

$T$ (°C)	Equation $\times 10^{-7}$	$R^2$
20	$D_{eff} = 0.0434v^2 - 0.529v + 3.6271$	0.996
30	$D_{eff} = 0.0237v^2 - 0.4616v + 4.1962$	0.9973
40	$D_{eff} = 0.2355v^2 - 1.8509v + 7.1562$	0.9967
50	$D_{eff} = 0.2229v^2 - 2.0047v + 8.9563$	0.9846
60	$D_{eff} = 0.2121v^2 - 2.2011v + 11.395$	0.9151

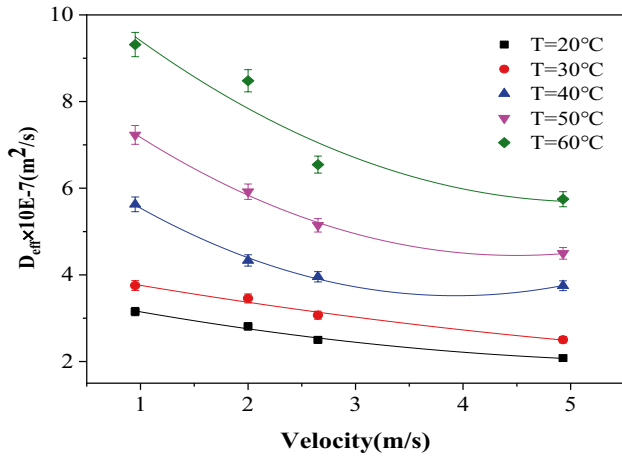


**Fig. 4**  $D_{eff}$  versus air velocity at different air temperatures for drying of shredded tobacco sample

$$D_{eff} = (1.371 - 0.112T + 0.375v + 4.474 \times 10^{-3}T^2 + 0.01vT + 0.188v^2 - 7.355 \times 10^{-5}T^3 - 3.817 \times 10^{-5}T^2v - 6.517 \times 10^{-3}Tv^2 - 0.026v^3 + 4.515 \times 10^{-7}T^4 + 1.228 \times 10^{-7}T^3v - 1.519 \times 10^{-5}T^2v^2 + 9.934 \times 10^{-4}Tv^3) \times 10^{-6} (R^2 = 0.9945)$$

### 3.3 Activation energy

The values of  $E_a$  are determined through Eq. (9) and the curve about the values of  $\ln(D_{eff})$  versus  $1/Ta$  shown in Fig. 6 is drawn by means of linear fitting.

The value of energy activation  $E_a$  lies in the general range of 12.7–110 kJ/mol for material drying process

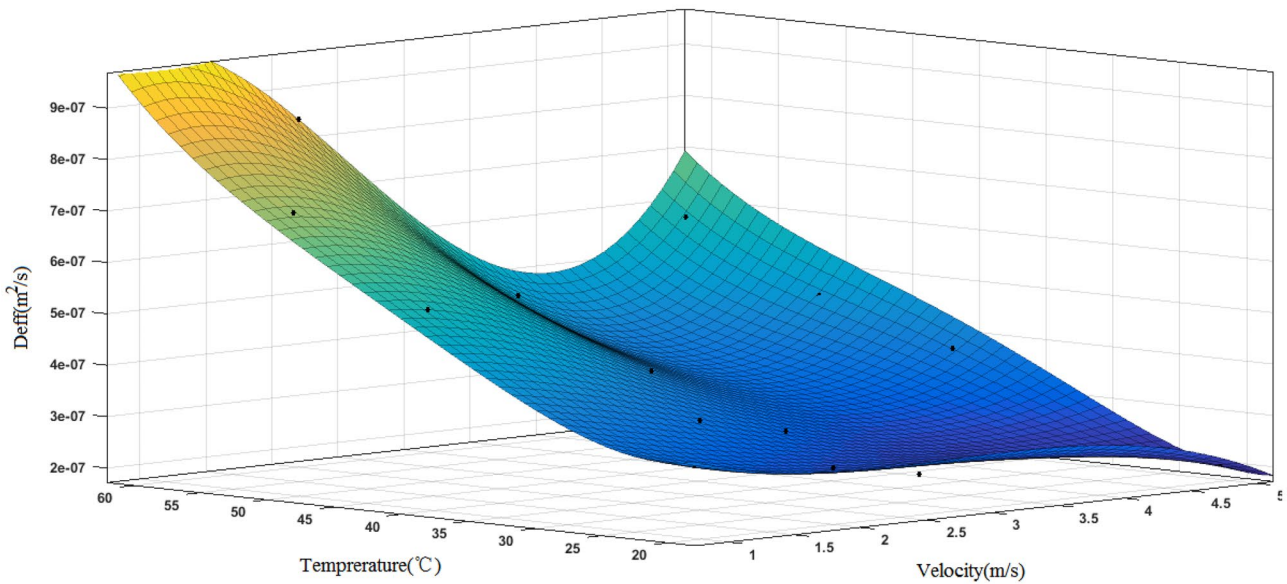


**Fig. 5** Influence of air temperature and velocity on  $D_{eff}$  during the shredded tobacco drying process

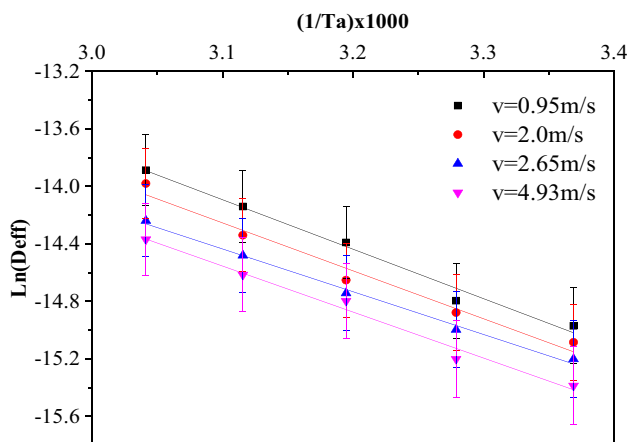


**Fig. 6**  $\ln(D_{eff})$  versus  $1/Ta$  for different air velocities during drying of shredded tobacco

[33]. Babalis et al. [34] reported  $E_a$  in the range of 30.8 to 48.47 kJ/mol for figs and Mortaza et al. [35] reported this value within the range of 110.837–130.61 kJ/mol for Berberis fruit. The values of  $E_a$  at different air velocities are contained in Table 3, it shows that the activation energy of shredded tobacco is within the range of 14.29 to 22.89 kJ/mol. It was found that the activation energy of tobacco in this study is similar to that in the references [23, 36]. However, it is lower than that reported in Ref. [17], with a maximum of 35.2 kJ/mol. It reflects the influence of tobacco types and sources on the results. Considering the low initial moisture which is found to be only 30% and the effects of other factors such as the form of shredded tobacco, tissue thickness, the infrequent structure of tobacco and intensive changes of  $D_{eff}$  value for different air temperatures at constant air velocity, the activation energy of shredded tobacco is lower when compared with other food products [37].

The activation energy values versus air velocity is plotted in Fig. 7. The maximum  $E_a$  value occurs when air velocity lies in 1.0–1.5 m/s and the minimum  $E_a$  occurs when air velocity lies in 3.5–4.0 m/s. On the other hand, the activation energy will increase while the air velocity above 4.0 m/s continues to increase. The three-order equation fitted with the calculated data is as follows:

$$E_a = 1.37996v^3 - 10.97538v^2 + 22.89642v + 9.77387 \tag{12}$$

**Table 3** The activation energy and correlation coefficient for different air velocities

$v(m/s)$	0.95	2.0	2.65	3.5	4.93
$E_a(kJ/mol)$	22.89	22.18	19.79	14.29	21.29
$R^2$	0.9822	0.9667	0.9931	0.9206	0.9808

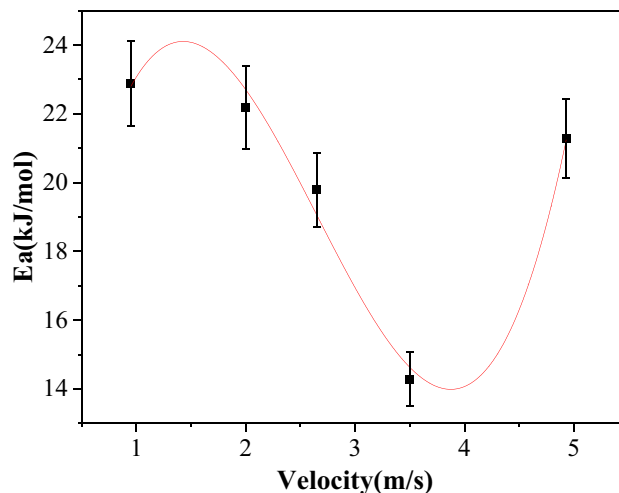


**Fig. 7** The influence of air velocity on activation energy value during tobacco drying

**Table 4** Mathematical models applied to the drying curves

Number	Model	Equation	References
1	Lewis	$MR = \exp(-kt)$	[8, 38]
2	Logarithmic	$MR = a \cdot \exp(-kt) + c$	[14, 39]
3	Midilli-Kucuk	$MR = a \cdot \exp(-kt) + bt$	[12, 40]
4	Henderson and pabis	$MR = a \cdot \exp(-kt)$	[41, 42]
5	Parabolic	$MR = a + bt + ct^2$	[43, 44]
6	Verma	$MR = a \cdot \exp(-kt) + (1 - a)\exp(-gt)$	[45, 46]

### 3.4 Modeling of the drying curves

To examine the drying kinetics at different drying conditions, several semi-theoretical thin-layer drying models in Table 4 are widely employed for determining the drying curves.

The most suitable model that describing the drying kinetics form of shredded tobacco is selected on the basis of the highest coefficient of determination ( $\phi^2$ ), the lowest mean bias error ( $e_{RMSE}$ ) and the lowest reduced chi-square ( $\chi^2$ ) [47]. These parameters are given as follows:

**Table 5** Statistical analysis results of the selected mathematical models

Models	$\phi^2$	$e_{RMSE}$	$\chi^2$
Lewis	0.8508	0.2780	0.0536
Logarithmic	0.9676	0.2322	0.0402
Midilli-Kucuk	0.9628	0.2471	0.0424
Henderson and pabis	0.9421	0.2427	0.0576
Parabolic	0.7679	0.2558	0.3060
Verma	0.8925	0.2516	0.0897

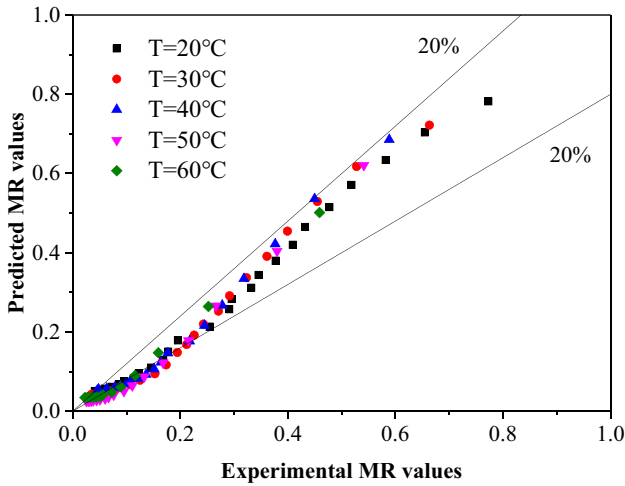


**Fig. 8** Comparison of the moisture ratio predicted by Logarithmic model and experimental data

**Table 6** Statistical analysis results of the proposed model

statistical parameters	$\phi^2$	$e_{RMSE}$	$\chi^2$
value	0.9990	0.0067	$5.7232 \times 10^{-5}$

$$\phi^2 = \frac{\sum_{i=1}^N (MR_{pre,i} - \overline{MR}_{exp})^2}{\sum_{i=1}^N (MR_{exp,i} - \overline{MR}_{exp})^2} \tag{13}$$

$$\chi^2 = \frac{\sum_{i=1}^N (MR_{exp,i} - MR_{pre,i})}{N - P} \tag{14}$$

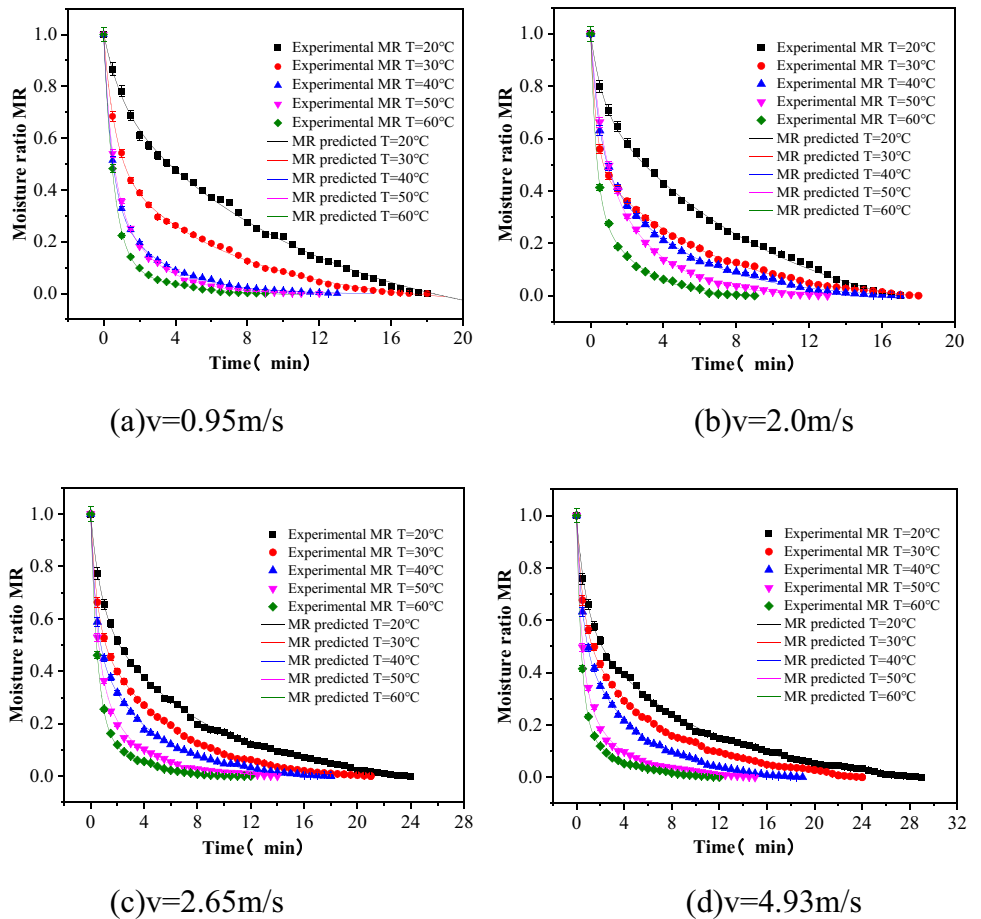
$$e_{RMSE} = \sqrt{\frac{\sum_{i=1}^N (MR_{pre,i} - \overline{MR}_{exp})^2}{N}} \tag{15}$$

where  $MR_{exp}$  is the moisture ratio in experiment and  $MR_{pre}$  is the predicted moisture ratio,  $N$  is the number of measurements,  $P$  is a constant number in a model and  $i$  is the number of terms.

Then, the selected empirical model is used to predict the moisture content under different working conditions. By comparing the predicted results with experimental data, the performance indicators of each model are calculated, which are shown in Table 5.

The results show that the logarithmic model has the largest  $\phi^2$  among the selected models. In addition, the logarithmic model has smaller  $e_{RMSE}$  and  $\chi^2$  than other models. It can be

**Fig. 9** Experimental data of moisture ratio versus drying time fitted with model





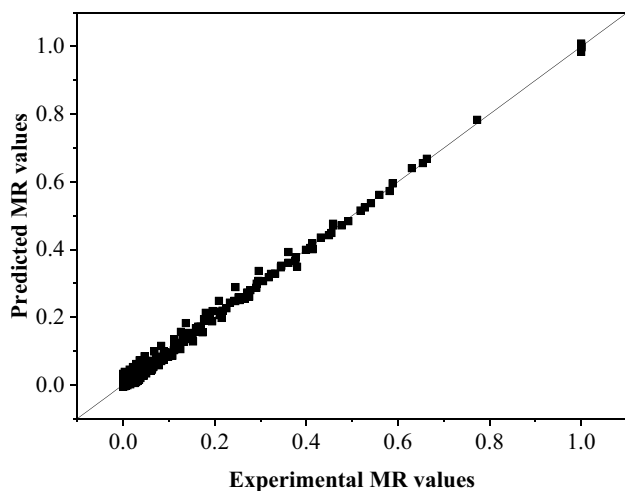


**Fig. 10** The predicted moisture ratio by the proposed model versus experimental data

seen that the logarithmic model is the most suitable model to predict the drying characteristics of tobacco, which is consistent with the results of literature [17].

Taking the air velocity of 2.65 m/s as an example, the comparison between the experimental MR value and the logarithmic model is shown in Fig. 8. As shown in Fig. 8, the Logarithmic model has a good prediction in the initial drying period. However, the prediction error of the model is over 20% in the later stage of drying.

In order to improve the prediction accuracy of tobacco drying characteristics, a new mathematical model is developed based on the Logarithmic model and the Two-term model. The expression of the proposed model is as follows:

$$MR = a \cdot \exp(-bt) + c \cdot \exp(-dt) + e \quad (16)$$

The experimental data are used to fit the proposed model, and the drying constants of the model under different conditions are obtained. The performance indicators used to evaluate the model are shown in Table 6.

From Table 6, the custom model has a high correlation coefficient value ( $\phi^2=0.999$ ), and a low value of  $e_{\text{RMSE}}$  and  $\chi^2(e_{\text{RMSE}}=0.0067, \chi^2=5.7232 \times 10^{-5})$ .

It can be seen from Figs. 9 and 10 that the moisture ratio predicted by the proposed model is in good agreement with experimental results at different drying temperatures. Therefore, the proposed model can be used to predict the drying kinetics characteristics of shredded tobacco in the drying equipment.

## 4 Conclusion

In this paper, an experimental equipment is developed to investigate the drying kinetics and modeling of shredded tobacco, different air temperatures (20, 30, 40, 50, 60 °C) and air velocities

(0.95, 2.0, 2.65, 4.93 m/s) are examined for the air drying process. Several mathematical drying models are analyzed for fitting the experimental data and a new predictive model is developed. The following conclusions can be drawn from the present work:

1. The effective moisture diffusivity increases with the increase of air temperature, while it decreases with the increase of air velocity. When the air velocity increases from 0.95 m/s to 4.93 m/s at the temperature of 60°C, the  $D_{\text{eff}}$  decreases by 39.31%. The activation energy of shredded tobacco varies from 14.29 to 22.89 kJ/mol.
2. Among several selected mathematical drying models, the Logarithmic model is the most suitable for shredded tobacco during the preliminary stage. However, this model has poor predictability in the late drying period and the maximum deviation is more than 20%.
3. A new prediction model based on Logarithmic and Two-term models is proposed. The highest coefficient of determination of the proposed model is 0.9990, which greatly improves the prediction accuracy of drying characteristics of tobacco.

This work provides a prediction model to evaluate drying characteristics of tobacco under different operation conditions. Based on this model, we will simulate the mass and heat transfer process of tobacco in different drying equipment in the next study. In addition, it is still a challenge to develop a high precision drying prediction model to accurately simulate the performance of tobacco drying equipment. With the development of artificial intelligence technology, a data-driven machine learning method is an effective way to address this challenge.

**Acknowledgements** This work was supported by the Natural Science Foundation of Hunan Province, China (Grant No.2022JJ30568, Grant No.2021JJ30677).

**Author contributions** Zhiqi Wang: Conceptualization, Methodology, Writing-original draft. Qianghui Yi: Experimental testing and data reduction. Xiaoxia Xia: Conceptualization, Writing-review & editing. Xin Li: Construction of experimental system, Experimental testing. Sifeng Zhang: Data curation, Formal analysis. Xiaoyue Zhang: Formal analysis, Writing-review. All authors discussed the results and contributed to the final manuscript. All authors have read and agreed to the published version of the manuscript.

**Data availability** The data are available from the corresponding author on reasonable request.

## Declarations

**Competing interests** The authors declare no competing interests.

## References

1. Hu A (2016) Research on the development of China's tobacco industry from the perspective of monopoly. Ph.D. Shandong university, Shangdong, China

2. Zongying W, Juncang P, Lei X et al (2012) Comparative analysis of leaf processing quality under two drying processes. *Tobacco Sci Technol* 11:5–9
3. Li Q, Li YF, Zhang Y et al (2017) Drying kinetics study of irregular fibril materials in a 'differential' laboratory rotary dryer: a case study for cut tobacco. *Drying Technol* 36(5):523–536
4. Taghian DS, Hamdami N, Shahedi M et al (2014) Mathematical modeling of hot air/electrohydrodynamic (EHD) drying kinetics of mushroom slices. *Energy Convers Manage* 86:70–80
5. Puente-dí'az L, Ah-Hen K, Vega-Ga' lvez A et al (2013) Combined infrared-convective drying of murta (*Ugni molinae* Turcz) berries: kinetic modeling and quality assessment. *Dry Technol* 31(3):329–338
6. Doymaz I (2012) Evaluation of some thin-layer drying models of persimmon slices (*Diospyros kaki* L.). *Energy Convers Manage* 56:199–205
7. Khazaei J, Arabhosseini A, Khosrobeigy Z (2008) Application of superposition technique for modeling drying behavior of *Avishan* (*Zataria multiflora*) leaves. *Trans ASABE* 51(4):1383–1393
8. Shi Q, Zheng Y, Zhao Y (2013) Mathematical modeling on thin-layer pump drying of yacon (*Smallanthus sonchifolius*) slices. *Energy Convers Manage* 71:208–216
9. Tođrul Tİ, Pehlivan D (2002) Mathematical modeling of solar drying of apricots in thin layers. *J Food Eng* 55(3):209–216
10. Midilli A, Kucuk H, Yapar ZA (2002) New model for single layer drying. *Dry Technol* 20(7):1503–1513
11. Zhiqiang G, Xiuzhi W, Min L, Jiang X, Xie J (2012) The thin-layer model of hot air drying of fruit pulp. *J Agric Mach* 43(02):151–158
12. Safa M, Mourad O, Nadia H et al (2017) Drying characteristics and kinetics solar drying of Moroccan rosemary leaves. *Renewable Energy* 108:303–310
13. Panchariya PC, Popovic D, Sharma AL (2002) Thin-layer modeling of black tea drying process. *J Food Eng* 52(4):349–357
14. Ashtiani SHM, Salarikia A, Golzarian MR (2017) Analyzing drying characteristics and modeling of thin layers of peppermint leaves under hot-air and infrared treatments. *Inf Process Agric* 4(2):128–139
15. Li JX, Dai XM, Zhang JJ et al (2013) Analysis of drying kinetics of cigarette raw materials. *Hubei Agric Sci* 52(23):5788–5790+5820. (in Chinese)
16. Duan K, Zhu WK, Chen Q et al (2014) Changes of water content and temperature of cut tobacco during drying at variable temperature. *Tobacco Sci Technol* 04:20–25. (in Chinese)
17. Xin YN, Zhang JW, Li B (2018) Drying kinetics of smoke strips at different temperature and relative humidity. *J Therm Anal Calorim* 132:1347–1358
18. Zhu WK, Wang L, Duan K, Chen LY, Li B (2015) Experimental and numerical investigation of the heat and mass transfer for cut tobacco during two-stage convective drying. *Dry Technol* 33(8):907–914
19. Gu C, Zhang X, Li B, Yuan Z (2014) Study on heat and mass transfer of flexible filamentous particles in a rotary dryer. *Powder Technol* 267:234–239
20. Nie GJ, Liu WF, Zhou HS et al (2022) Numerical simulation of tobacco drying process in roller. *Tobacco Sci Technol* 55(12):80–87. (in Chinese)
21. Xie SL, Du JS, Lu DF et al (2019) Characterization of thermal working strength based on laboratory batch drum drying device and its influence on physical properties of tobacco. *Tobacco Sci Technol* 53(06):89–95. (in Chinese)
22. Liu JH, Zhu Y, Shen XF et al (2014) Effect of different steam injection positions on air dried tobacco quality. *Tobacco Sci Technol* 11:10–13+21. (in Chinese)
23. Liu W, Chen M, Liu H et al (2023) Isothermal drying characteristics and kinetic mechanism for tobacco with different water content. *BioResources* 18(2):2611–2626
24. Jiang S (2023) Heat and Mass transfer of filamentous materials in vacuum freeze-drying. *Yanshan University* (in Chinese)
25. Duan K, Zhao YZ, Lu CT et al (2017) Effects of convection drying on Surface Temperature and Physicochemical Properties of tobacco. *Food Mach* 33(10):184–189. (in Chinese)
26. Zhang XL, Zhou PF. Research and analysis of heat pump drying tobacco //Zhejiang Energy Research Association, Zhejiang Zheneng Technology Research Institute. Supply-side Structural Reform Leads Energy Transformation and Innovation -- Proceedings of the 13th Yangtze River Delta Energy Forum. Institute of Cold Storage Technology, Shanghai Maritime University; 2016–6. (in Chinese)
27. Aktas M, Sevik S, Aktekel B (2016) Development of heat pump and infrared-convective dryer and performance analysis for stale bread drying. *Energy Convers Manage* 113:82–94
28. Borah A, Hazarika K, Khayer SM (2015) Drying kinetics of whole and sliced turmeric rhizomes (*Curcuma longa* L.) in a solar conduction dryer. *Inf Process Agric* 2(2):85–92
29. Dehghannya J, Hosseinlar SH, Heshmati MK (2018) Multi-stage continuous and intermittent microwave drying of quince fruit coupled with osmotic dehydration and low temperature hot air drying. *Innov Food Sci Emerg Technol* 45:132–151
30. Fan K, Chen L, He J, Yan F (2015) Characterization of thin layer hot air drying of sweet potatoes (*Ipomoea batatas* L.) slices. *J Food Process Preserv* 39(6):1361–1371
31. Serowik M, Figiel A, Nejman M et al (2018) Drying characteristics and properties of microwave-assisted spouted bed dried semi-refined carrageenan. *J Food Eng* 221:20–28
32. Tao Y, Wang P, Wang Y et al (2016) Power ultrasound as a pretreatment to convective drying of mulberry (*Morus alba* L.) leaves: Impact on drying kinetics and selected quality properties. *Ultrason Sonochem* 31:310–318
33. Xiao HW, Yao XD, Lin H, Yang WX, Meng JS, Gao ZJ (2012) Effect of SSB (superheated steam blanching) time and drying temperature on hot air impingement drying kinetics and quality attributes of yam slices. *Food Process Eng* 35(3):370–390
34. Babalis SJ, Belessiotis VG (2004) Influence of drying conditions on the drying constants and moisture diffusivity during the thin-layer drying of figs. *J Food Eng* 65(3):449–458
35. Aghbashlo M, Kianmehr MH, Samimi-Akhijahani H (2008) Influence of drying conditions on the effective moisture diffusivity, energy of activation and energy consumption during the thin-layer drying of berberis fruit (*Berberidaceae*). *Energy Convers Manage* 49(10):2865–2871
36. Liu Z, Li B, Yu CF (2009) Dynamic analysis of combined heat transfer on enhanced mass transfer of thin layer tobacco. *Tobacco Sci Technol* 11:5–10
37. Gaware TJ, Sutar N, Thorat BN (2010) Drying of Tomato Using Different Methods: Comparison of Dehydration and Rehydration Kinetics. *Drying Technol* 28(5):651–658
38. Ocallahan J, Menzies D, Bailey P (1971) Digital simulation of agricultural dryer performance. *J Agric Eng Res* 16:223–244
39. Balasubramanian S, Sharma R, Gupta RK et al (2011) Validation of drying models and rehydration characteristics of betel (*Piper betel* L.) leaves. *J Food Eng* 48(6):685–691
40. Arslan D, Ozcan MM, Menges HO (2010) Evaluation of drying methods with respect to drying parameters, some nutritional and color characteristics of peppermint (*Mentha x piperita* L.). *Energy Convers Manage* 51(12):2769–2775
41. Wang SY, Zhang K, Wang L et al (2021) Study on isothermal drying kinetics of remanufactured tobacco leaves with different processes of heating cigarettes. *Tobacco Sci Technol* 54(09):80–89. (in Chinese)

42. Xiao Y D, Wu H H, Tian Z et al (2023) Study on optimization of microwave-hot air drying process and drying kinetics of chives leaves. *Agric Process* 14:6-12. (in Chinese)
43. Wu JN, Chen XT, Pan N et al (2019) Drying characteristics and mathematical models of hippocampus under different drying methods. *Modern Food Sci Technol* 36(12):133-142. (in Chinese)
44. Zhang J (2023) Study on vacuum drying characteristics and model of Yam slices. Southwest University (in Chinese)
45. Lan DW, Zhao F, Wang YQ et al (2022) Study on Effect of hot air drying condition on drying characteristics and Mathematical model [J]. *Inner Mongolia Petrochem Ind* 48(04):54-58. (in Chinese)
46. Liu YF, Tan AL, Pan XL et al (2021) Research on mathematical model of microwave-vacuum thin layer drying of longan pulp [J]. *Anhui Agric Sci* 49(04):182-185. (in Chinese)
47. Kucuk H, Kilic A, Midilli A (2014) Common applications of thin layer drying curve equations and their evaluation criteria. Springer International Publishing 669–680

**Publisher's Note** Springer Nature remains neutral with regard to jurisdictional claims in published maps and institutional affiliations.

Springer Nature or its licensor (e.g. a society or other partner) holds exclusive rights to this article under a publishing agreement with the author(s) or other rightsholder(s); author self-archiving of the accepted manuscript version of this article is solely governed by the terms of such publishing agreement and applicable law.